Hindawi Publishing Corporation
Journal of Nanomaterials
Volume 2015, Article ID 526249, 5 pages
http://dx.doi.org/10.1155/2015/526249

Research Article

Ferroelectric and Dielectric Properties of $ZnFe_2O_4$-$Pb(ZrTi)O_3$ Multiferroic Nanocomposites

Shrabanee Sen, Sk. Md. Mursalin, and M. Maharajan

Sensor & Actuator Division, Central Glass and Ceramics Research Institute, 196 Raja SC Mullick Road, Kolkata 700032, India

Correspondence should be addressed to Shrabanee Sen; shrabanee@cgcri.res.in

Received 8 April 2014; Accepted 3 September 2014

Academic Editor: Debasis Dhak

Magnetoelectric composites of zinc ferrite and soft lead zirconate titanate (PZT) having formula 0.5 $ZnFe_2O_4$-0.5 PZT were synthesized by sol-gel technique. X-ray diffraction analysis was carried out to confirm the coexistence of individual phase. TEM micrographs were taken to confirm the formation of nanosized powders and SEM micrographs were taken to study the morphology of the sintered pellets. Dielectric and P-E hysteresis loops were recorded, respectively, to confirm the ferroelectric properties of the composites.

1. Introduction

The multiferroics are functional materials combining several ferroic properties in the same material. They usually exhibit simultaneously magnetic and ferroelectric order and a coupling between them. In recent years much attention has been given for the development of magnetoelectric materials due to their possible applications as sensors, memories, transducers, and actuators. One of the important classes of magnetoelectric materials includes ferrite piezoelectric composites. In such materials the magnetoelectric effect is a product property that depends on the piezoelectric and piezomagnetic coefficients, volume fraction of composite components, and magnetic, dielectric properties of composite components. The suitable combination of two phases such as piezomagnetic or magnetostrictive and piezoelectric phase can yield a desirable ME property [1–3]. Till date various ME composites have been prepared consisting of ferroelectric materials like $BaTiO_3$, $Pb(Zr)TiO_3$, $BaPbTiO_3$, and so forth and Ni, Co, Mg, Zn ferrites as magnetic phase [4–6]. The main advantage of synthesizing sintered ME composites is related to the easy and cheap fabrication and the possibility to control the molar ratios of phases, grain size, and densification.

For the present work, nanocomposites of 0.5 $ZnFe_2O_4$-0.5 soft $Pb(ZrTi)O_3$ were prepared by the sol-gel method and the structural, microstructural, and dielectric properties were studied and compared with the parent compound, that is, PZT.

2. Experiment

2.1. Material Synthesis. The nanocomposites were prepared by a two-step technique. In the first step $ZnFe_2O_4$ nanopowders were prepared by a sol-gel technique. The precursor materials for $ZnFe_2O_4$ were $Zn(NO_3)_2{\cdot}6H_2O$ (Aldrich) and $Fe(NO_3)_3{\cdot}9H_2O$ (Aldrich). At first, the stoichiometric amount of $Zn(NO_3)_2{\cdot}6H_2O$ and $Fe(NO_3)_3{\cdot}9H_2O$ was taken in a beaker, and a complete homogeneous solution was prepared in 200 mL of distilled water. This prepared solution was then stirred for 1 h. During the stirring, equimolar amount of citric acid was added to the solution. To that solution, soft lead zirconate titanate, that is, PZT (Sparkler ceramics), dissolved in nitric acid was added and the stirring was continued for more than 4 h, keeping the temperature in the range of 100 to 110°C. After that, finally a heavily dense form of the sol has been obtained. The sol was then put into the oven at 110°C and was left for 10 h to form a hard gel. The precursor powders were calcined for ~8 h at 500°C.

The powders were further reground thoroughly, pelletized, and sintered at 1250°C (2 h) in presence of excess

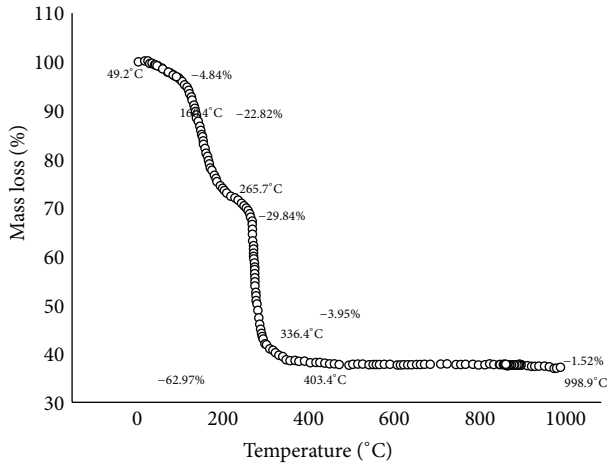

Figure 1: TGA of $ZnFe_2O_4$-PZT gel.

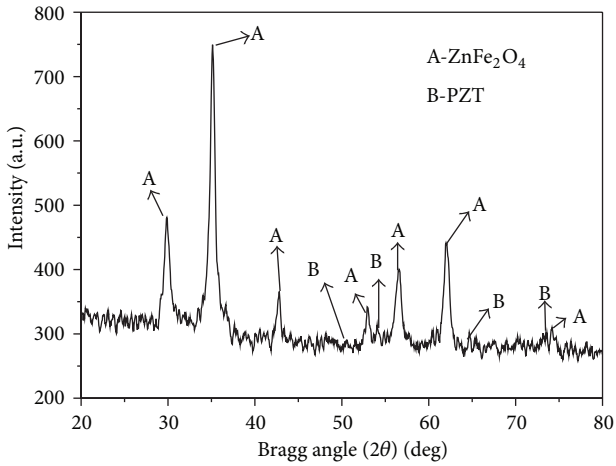

Figure 2: XRD of $ZnFe_2O_4$-PZT nanopowders.

lead oxide to obtain pellets required for characterization of electrical properties.

2.2. Characterization. Thermal analysis of the dried gel in air was done using Perkin Elmer Thermal Analyzer from 30°C to 1000°C at the heating rate of 10°C/min. The powder X-ray diffraction of synthesized $ZnFe_2O_4$powder was carried out using Bruker AXS D8 Advance system (λ = 1.5406 Å, with a step size of 0.05°). The morphology of the nanopowders was observed by Transmission Electron Microscope (Techno $G^2$30 STWin) and the pellets were observed on a Field Emission Scanning Electron Microscope (SUPRA 35 VP) at different magnifications. For electrical measurements the pellets were polished and electroded with silver paint. The dielectric properties were measured by a LCR meter (Hioki 3532) as a function of frequency and temperature and the ferroelectric properties as a function of voltage were measured with Aixact Test Bench.

3. Results and Discussion

Figure 1 shows the thermal plot of $ZnFe_2O_4$-PZT gel. Since commercial PZT powder (Sparkler ceramics) was used and mixed, the plot is more or less identical to that of $ZnFe_2O_4$ reported [7, 8]. The weight loss in the range 200°C–250°C in the TGA curve attributed to the liberation of surface adsorbed water. The drastic weight loss corresponds to the conventional oxidative decomposition of citric acid and nitrates. The redox reaction between citric acid, metal nitrates, and PZT mixture has completed above 400°C, indicating the completion of the decomposition of citric acid and nitrate salts. No weight loss above 400°C suggests the formation of crystalline 0.5 $ZnFe_2O_4$-0.5 PZT as the decomposition product.

The XRD pattern of $ZnFe_2O_4$-PZT calcined at 500°C/8 h is shown in Figure 2. The formation of $ZnFe_2O_4$-PZT powder was confirmed by matching the peak position with the JCPDS file $ZnFe_2O_4$ (PDF-821042) and soft PZT which is given in the inset. Hence formation of multiferroic composite was confirmed from structural characterization. The mean crystallite size of the powder was calculated using Scherrer formula and was found to be ~28 nm.

Figure 3(a) shows the TEM micrographs of 0.5 $ZnFe_2O_4$-0.5 PZT nanocomposite. The average particle size estimated was ~35 nm. HRTEM micrographs (Figure 3(b)) show the perfect orientation of the lattice spacing and SAED pattern (Figure 3(c)) depicts the formation of distinct rings which confirms the formation of crystalline nature of the sample. The EDAX micrograph (Figure 3(d)) confirms that both the ferroelectric compound (PZT) and the ferromagnetic $ZnFe_2O_4$ nanocrystals are present in the composite. Hence formation of multiferroic composite was confirmed. The atomic percentages of all the elements are given in Table 1.

FESEM micrographs of 0.5 $ZnFe_2O_4$-0.5 PZT pellet at different magnifications (5 and 10 KX) and at different selected areas are shown in Figures 4(a) and 4(b). The homogeneous distribution of the grains of average size of 6–8 μm with hexagonal shape having distinct grain boundaries is confirmed from the micrographs. Densely packed grains

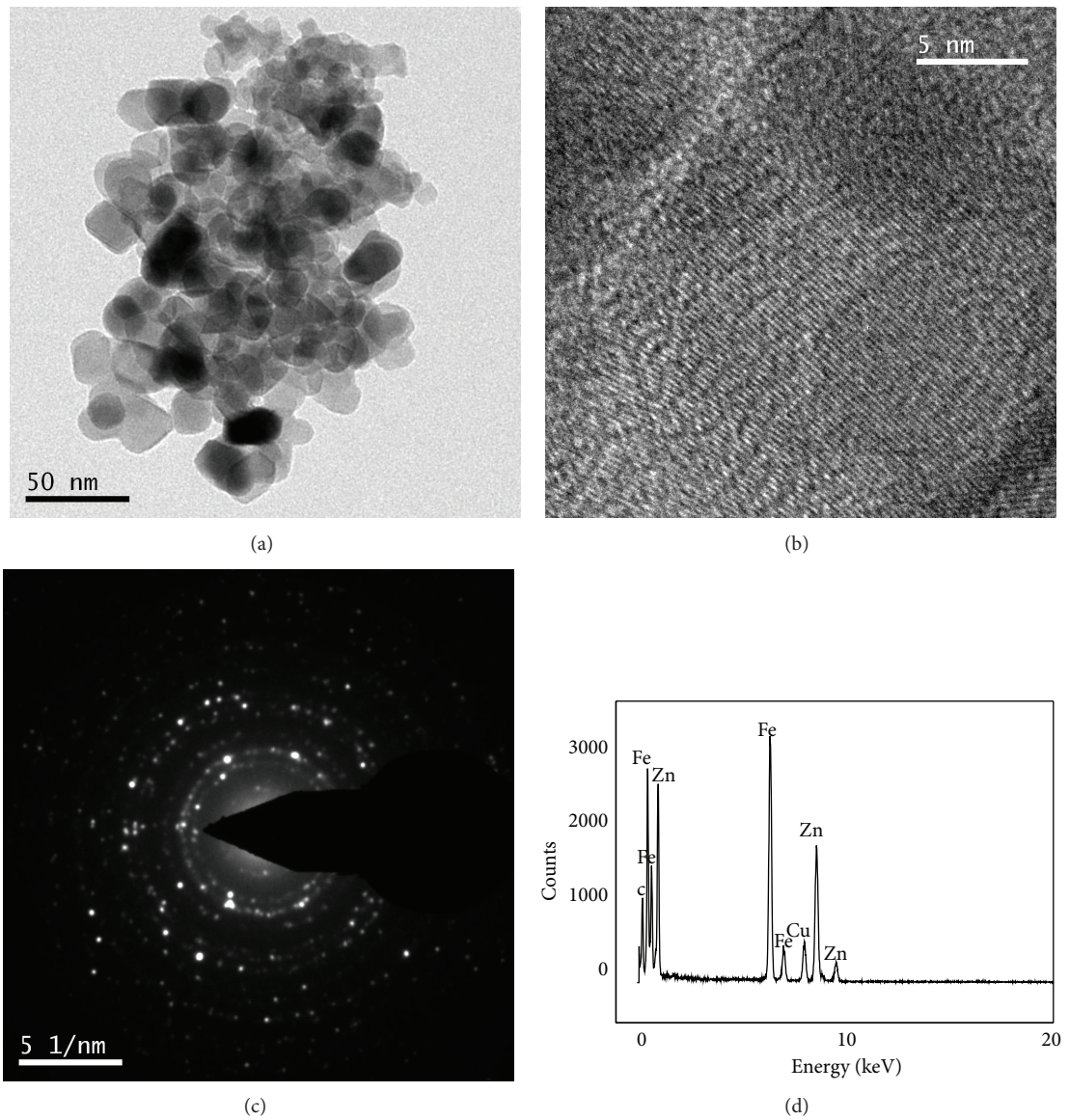

Figure 3: (a) TEM micrographs. (b) HRTEM micrographs. (c) SAED micrographs. (d) EDAX micrographs.

Table 1: Elemental analysis of $ZnFe_2O_4$-PZT composite.

Element	Weight %	Atomic %	Uncert. %	Correction	k-factor
O(K)	29.40	63.56	0.32	0.49	1.973
Ti(K)	0.09	0.06	0.01	0.98	1.193
Fe(K)	34.13	21.14	0.24	0.99	1.348
Zn(K)	23.75	12.56	0.23	0.99	1.671
Zr(K)	2.60	0.98	0.10	0.99	3.439
Pb(L)	10.00	1.67	0.23	0.75	5.806

with relative high density (>95%) were observed from these micrographs.

The variation of dielectric constant (ε) and dielectric loss ($\tan\delta$) from 50 Hz to 5 MHz with variation from RT to 300°C is shown in Figures 5(a) and 5(b). It has been observed that, with the increase of frequency, ε value decreases and further remains almost constant. At lower frequencies all the polarization (i.e., electronic, ionic, dipolar, and interfacial) is present but at higher frequencies only the electronic polarization contributes to the dielectric constant. The value of the dielectric constant was less compared to that of the soft PZT which shows the effect of addition of $ZnFe_2O_4$. The dielectric loss decreased with the increase in frequency which is the general characteristics of a ferroelectric material. The variation of dielectric constant and tangent loss with temperature of the composite is shown in Figures 6(a) and 6(b). It is observed that the compounds do not exhibit phase transition up to the possible measurable temperature, that is, 300°C. There is a linear increase in both values within the measured temperature range. The dielectric constant value

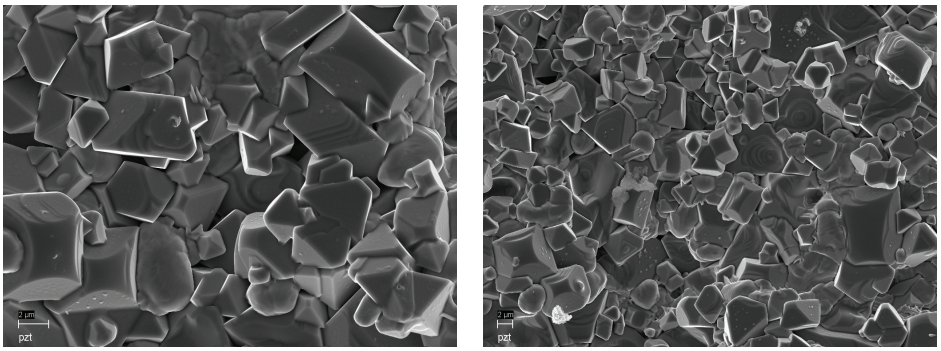

(a) (b)

Figure 4: (a) FESEM micrographs at 10 KX magnification of $ZnFe_2O_4$-PZT pellet. (b) FESEM micrographs at 5 KX magnification of $ZnFe_2O_4$-PZT pellet.

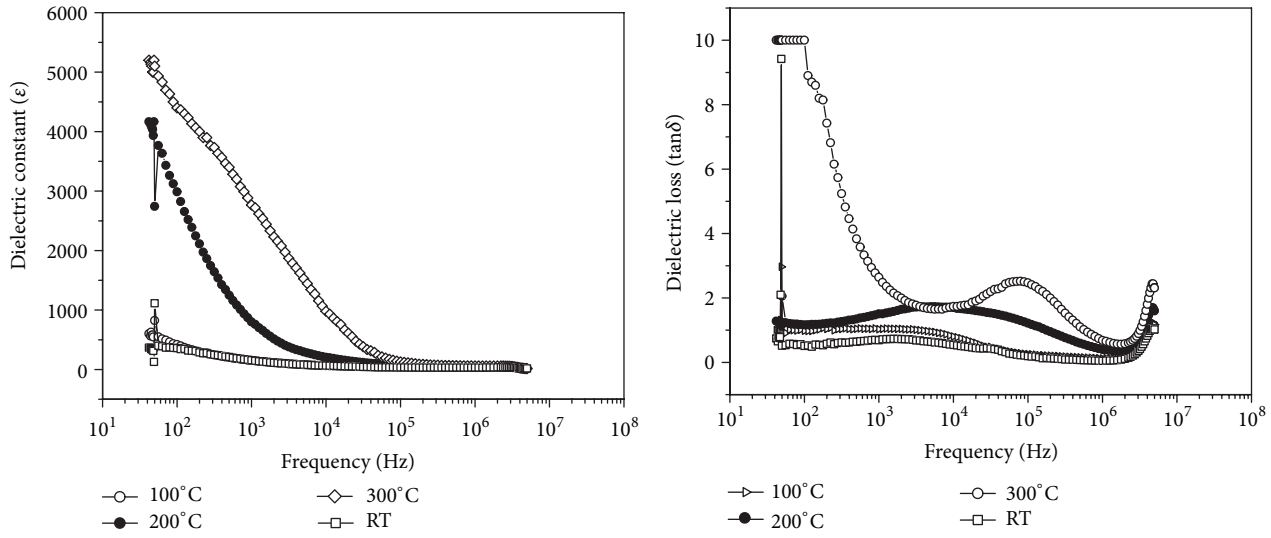

(a) (b)

Figure 5: (a) Variation of dielectric constant with frequency at different temperatures. (b) Variation of dielectric loss with frequency at different temperatures.

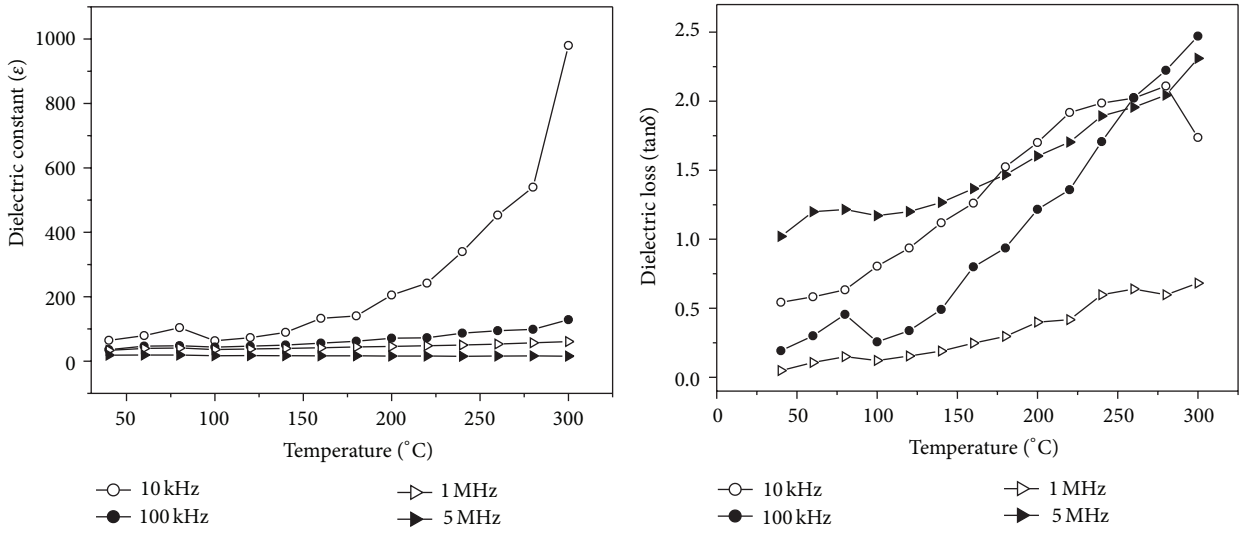

(a) (b)

Figure 6: (a) Variation of dielectric constant with temperature at different frequencies. (b) Variation of dielectric loss with temperature at different frequencies.

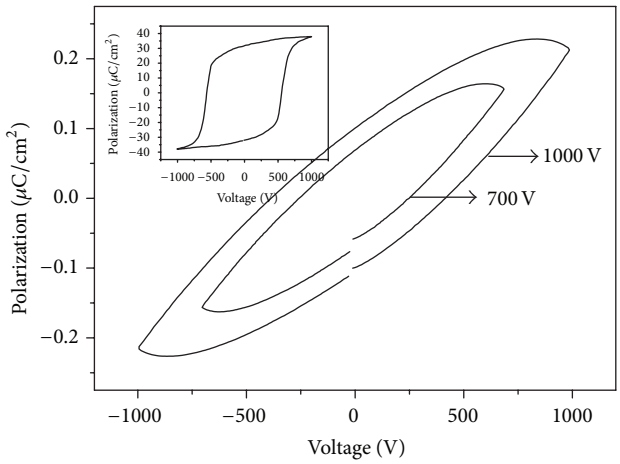

Figure 7: P-E loops of $ZnFe_2O_4$-PZT pellet compared with PZT pellet.

has decreased in comparison to soft PZT (PZT (RT) at 10 kHz = 1800).

Figure 7 shows the P-E hysteresis curve of the composite at room temperature. The remanent polarization (P_r) nanocomposite was 4 μC/cm^2 applied voltage of 1 Kv while that of soft PZT was 25 μC/cm^2. The similar loop of PZT sample is shown in the inset. The high reduction in the polarization value may be due to the interaction of the $ZnFe_2O_4$ grains which results in the pinning effect of the ferroelectric domains.

4. Conclusions

ZF-PZT composites were synthesized by sol-gel technique and were characterized by XRD, TEM, and SEM for structural and microstructural analysis. The dielectric constant decreased with respect to PZT. The observation of P-E hysteresis loops indicates the presence of ordered ferroelectric behaviour.

Conflict of Interests

The authors declare that there is no conflict of interests regarding the publication of this paper.

Acknowledgments

The authors would like to acknowledge Dr. K. Dasgupta (Director at CGCRI-CSIR) and Dr. A. Sen (Head at Sensor and Actuator Division) for giving permission for publishing this paper.

References

[1] R. F. Gibson, *Principles of Composite Material Mechanics*, McGraw-Hill, 1994.

[2] M. Taya, *Electronic Composites: Modeling, Characterization, Processing, MEMS Applications*, Cambridge University Press, Cambridge, UK, 2007.

[3] J. Van Suchetelene, "Product properties: a new application of composite materials," *Philips Research Reports*, vol. 27, pp. 28–37, 1972.

[4] R. Rani, J. K. Juneja, S. Singh, K. K. Raina, and C. Prakash, "Study of $0.1Ni_{0.8}Zn_{0.2}Fe_2O_4$–$0.9Pb_{1-3x/2}LaxZr_{0.65}Ti_{0.35}O_3$ magnetoelectric composites," *Journal of Magnetism and Magnetic Materials*, vol. 325, pp. 47–51, 2013.

[5] H.-F. Zhang, S. W. Or, and H. L. W. Chan, "Electrical, magnetic, and magnetoelectric characterization of fine-grained $Pb(Zr_{0.53}Ti_{0.47})O_3$-$(Ni_{0.5}Zn_{0.5})Fe_2O_4$ composite ceramics," *Journal of Alloys and Compounds*, vol. 509, no. 21, pp. 6311–6316, 2011.

[6] C. E. Ciomaga, M. Airimioaei, V. Nica et al., "Preparation and magnetoelectric properties of $CoFe_2O_4$–$Pb(ZrTi)O_3$ composites obtained in-situ by gel combustion method," *Journal of the European Ceramic Society*, vol. 32, p. 3325, 2013.

[7] M. Maharajan, M. D. Mursalin, M. Narjinary, P. Rana, S. Sen, and A. Sen, "Synthesis, characterization and vapour sensing properties of nanosized $ZnFe_2O_4$," *Transactions of the Indian Ceramic Society*, vol. 73, no. 2, pp. 102–104, 2014.

[8] M. Veith, M. Haas, and V. Huch, "Single source precursor approach for the sol-gel synthesis of nanocrystalline $ZnFe_2O_4$ and zinc-iron oxide composites," *Chemistry of Materials*, vol. 17, no. 1, pp. 95–101, 2005.